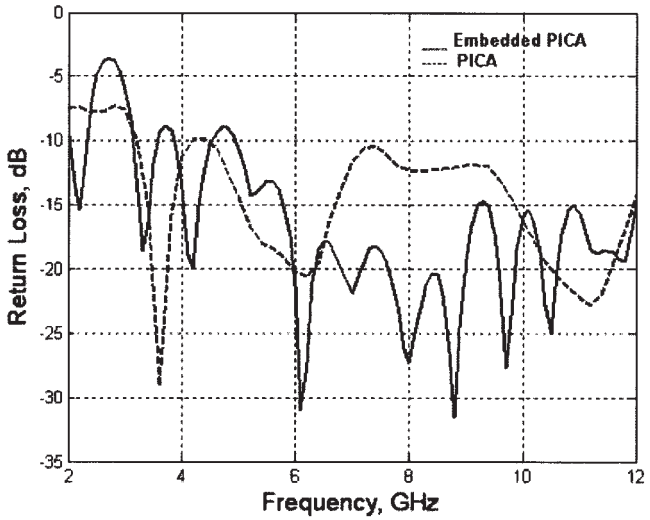

Figure 4 Measured return loss

REFERENCES

1. P. Agrawall, G. Kumar, and K.P. Ray, Wide-band planar monopole antenna, IEEE Trans Antenn Propag 46 (1998), 294–295.
2. S.Y. Suh, W.L. Stutzman, and W.A. Davis, A new ultrawideband printed monopole antenna: The planar inverted cone antenna (PICA), IEEE Trans Antenn Propag (2004), 1361–1364.
3. X. Qing, Z.N. Chen, and M.Y.W. Chia, Network approach to UWB antenna transfer functions characterization, In: 35th European Microwave Conference, Paris, October 4–6, 2005, pp. 1751–1754. Institute for Infocomm Research, Singapore.
4. E. Guillanton, J.Y. Dauvignac, C. Pichot, and J. Cashman, A new design tapered slot antenna for ultra-wide band applications, Mircow Opt Tech Lett 19 (1998), 286–289.
5. S.H. Choi, J.K. Park, S.K. Kim, and J.Y. Park, A new ultra-wide band antenna for UWB applications, Mircow Opt Tech Lett 40 (2005), 399–401.
6. J. Liang, C.C. Chiau, X. Chen, and C.G. Parini, Study of a printed circular disc monopole antenna for UWB systems, IEEE Trans Antenn Propag 53 (2005), 3500–3504.
7. Schantz, H. Planar elliptical element ultra-wideband dipole antennas, IEEE Antenn Propag Soc Int Symp 3 (2002), 16–21.
8. S. Gupta, M. Ramesh, and A.T. Kalghatgi, Design of optimized CPW fed monopole antenna for UWB applications, In: 17th Asia Pacific Microwave Conference (APMC 2005), Suzhou, China, December 4–7, 2005.
9. J. Powell and A. Chandrakasan. Differential and single ended elliptical antennas for 3.1–10.6 GHz ultra wideband communication, Proc IEEE Antenn Propag Soc Int Symp, 3 (2004), 2935–2938.
10. S. Gupta, M. Ramesh, and A.T. Kalghatgi, Compact planar inverted conical antenna for UWB applications, In: European Microwave Conference, Manchester, September 10–17, 2006.

MAGNETIC LOADING OF EBG AMC GROUND PLANES AND ULTRATHIN ABSORBERS FOR IMPROVED BANDWIDTH PERFORMANCE AND REDUCED SIZE

D. J. Kern and D. H. Werner
Department of Electrical Engineering
Pennsylvania State University
University Park, PA 16802

Received 25 April 2006

ABSTRACT: *This paper demonstrates the advantages of magnetic loading within the substrate of an electromagnetic bandgap (EBG) surface. A conventional EBG surface has been shown to act as an artificial magnetic conductor over a narrow bandwidth. This paper demonstrates that by magnetic loading of the substrate, increased operating bandwidth is achieved for each resonant frequency. In addition, previous research has revealed that an ultrathin electromagnetic absorber design can be obtained by introducing loss into the frequency selective surface of an EBG absorber. It is now shown that a further reduction in thickness is possible by including a small amount of magnetic permeability within the dielectric substrate material.* © 2006 Wiley Periodicals, Inc. Microwave Opt Technol Lett 48: 2468–2471, 2006; Published online in Wiley InterScience (www.interscience.wiley.com). DOI 10.1002/mop.21972

Key words: *electromagnetic bandgap surface; metaferrite; artificial magnetic conductor; frequency selective surface; ultrathin absorber*

1. INTRODUCTION

Electromagnetic bandgap (EBG) structures have recently been used as artificial magnetic ground planes and ultrathin absorbers. An effective EBG artificial magnetic conductor (AMC) structure is one that achieves a reflection phase of zero degrees at the desired operating frequency. This has been accomplished previously using a genetic algorithm (GA) optimization for both single-band and multiband designs [1]. In both cases, one of the main limitations for these designs is the intrinsic narrowband response. The designs presented in this paper, however, take the GA optimization a step further by introducing a small amount of magnetic material into the substrate which acts to increase the operating AMC bandwidth significantly at all resonant frequencies.

Previously, it was shown that absorber thickness can be considerably reduced with respect to that of a standard Salisbury screen by using a Gangbuster Frequency Selective Surface (FSS) and a separate resistive sheet placed above the ground plane [2–4]. More recently it was demonstrated that the resistive sheet could be incorporated directly into the FSS structure by adding an appropriate amount of ohmic loss to the metallic screen [5]. On the basis of this observation, a robust GA optimization procedure was then developed and applied to design ultrathin EBG absorbers with a total thickness on the order of $\lambda/50$ or less.

Recently, a design methodology was presented to create a high-frequency artificial ferrite material, or metaferrite, by using an appropriately designed EBG surface [6]. A standard EBG surface was shown to be equivalent to a thin PEC backed slab of magnetic material with a frequency dependent permeability. The use of a GA demonstrated the ability to obtain low-loss metaferrite structures with a wide range of both positive and negative permeabilities.

Furthermore, by optimizing for appropriate loss in the FSS surface and dielectric substrate, the metaferrite can act as an

TABLE 1 EBG AMC Design Parameters With and Without Magnetic Loading

	No Loading	Magnetic Loading
Unit cell size (cm)	2.38 × 2.38	2.38 × 2.38
Thickness (mm)	5.08	5.08
Permittivity	36.00	30.79
Permeability	1.00	3.90
Bandwidth		
860 MHz	5.33%	23.00%
1.575 GHz	2.64%	9.40%
1.876 GHz	1.68%	2.70%

electromagnetic absorber at the desired operating frequency. The metaferrite optimization procedure provides a much more intuitive approach to the design of EBG absorbers. This technique has been further generalized in this paper to include the use of magnetic material in the design of EBG absorbing surfaces. This allows for increased bandwidth for a given absorber thickness, or a thinner absorber for a minimum bandwidth requirement. These results are presented in Section 3.

2. GA APPROACH

In this section, a brief overview of the GA optimization approach is given. The use of a GA allows for simultaneous optimization of the unit cell size, dielectric permittivity, permeability and thick-

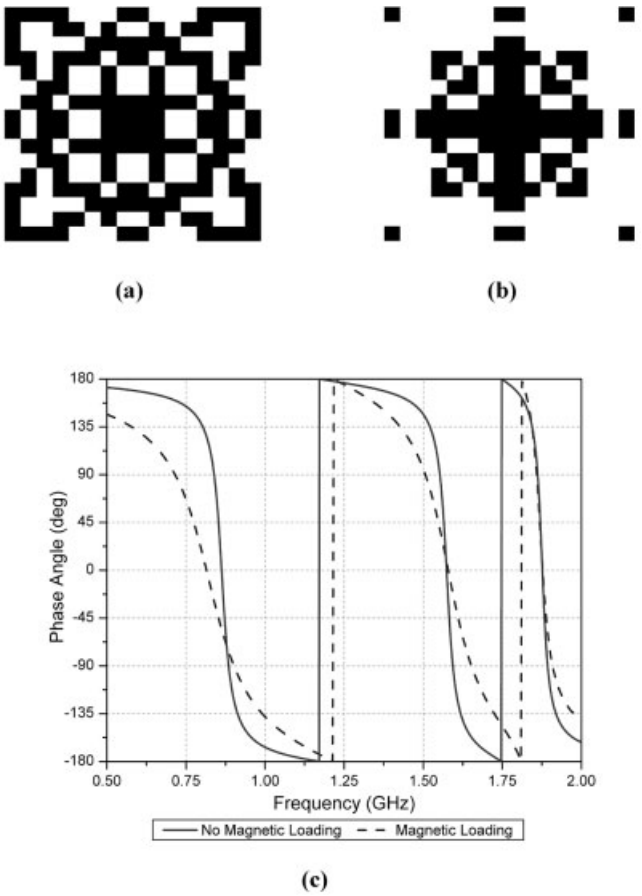

Figure 1 Triband EBG AMC designs with and without magnetic loading. Unit cell geometry without magnetic loading (a), unit cell geometry with magnetic loading (b), and reflection phase response for both (c)

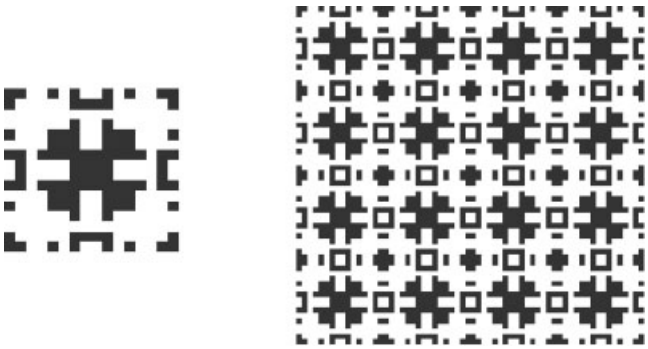

Figure 2 Unit cell geometry and corresponding FSS screen geometry for an ultrathin electromagnetic bandgap absorber with magnetic substrate

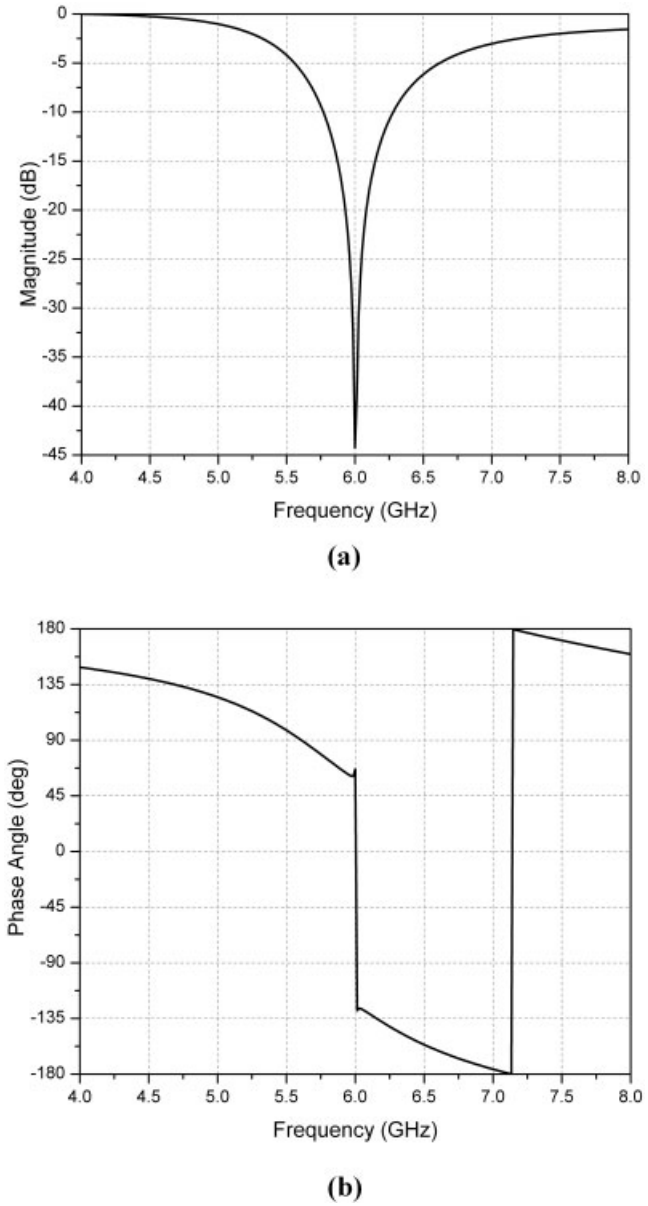

Figure 3 Frequency response of the ultrathin EBG absorber. Reflection coefficient magnitude versus frequency (a), and reflection phase angle versus frequency (b)

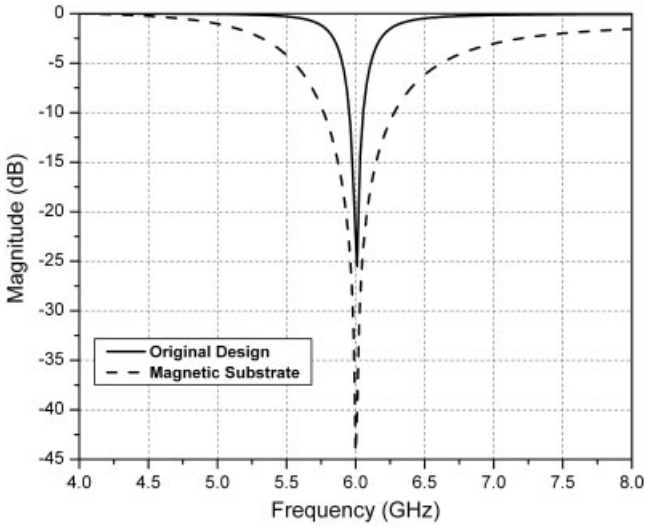

Figure 4 Reflection coefficient magnitude versus frequency for the previous ultrathin EBG absorber design with no magnetic substrate compared with the improved design with magnetic permeability. The improved design has a larger bandwidth and is thinner than the previous design

ness, FSS screen geometry, as well as the resistive component of the FSS screen when optimizing absorbers.

In the case of GA-optimized EBG AMC surfaces, the fitness function is relatively simple. When the system has no loss, the reflection coefficient will always have a magnitude of unity, and therefore only the phase term is required for optimization. The fitness function is given by

$$\mathrm{FF} = -\mathbf{max}(\phi_{\mathrm{TE}},\phi_{\mathrm{TM}}). \tag{1}$$

In this case, the GA selects the largest of the two phase angles and makes that number negative. The next generation looks for a smaller maximum phase angle, which results in a larger, but still negative, value of the fitness function. Thus, the GA uses a maximizing fitness function with a best solution having a maximum value of zero. A similar GA technique was previously employed in [1] to design the original single-band and multiband EBG surfaces without magnetic loading.

The fitness function used in the GA for synthesizing a lossy EBG absorber is given by

$$\mathrm{FF} = \frac{1}{0.2|\phi_{\mathbf{max}}/180| + 0.8|\Gamma_{\mathbf{max}}|}, \tag{2}$$

where $\Gamma_{\mathbf{max}}$ and $\phi_{\mathbf{max}}$ (in degrees) are the maximum reflection coefficient magnitude and phase, respectively. For optimizing multiple frequencies, the fitness function in Eq. (2) was simply calculated for each resonance and added together to create the final fitness function.

3. MAGNETIC LOADED EBG RESULTS

The first result presented here is a triband EBG AMC surface optimized for maximum bandwidth [7]. This structure was designed for operation at 860, 1.575, and 1.88 GHz using a GA. Table 1 lists the parameters for the first design, constrained to have a relative permeability of 1.0, as well as the second design, which uses magnetic loading. The percent bandwidths are also given in this table, and are shown to decrease with increasing resonant frequency.

TABLE 2 6-GHz EBG Absorber Design Parameters With and Without Magnetic Loading

	Original Design	Design With Magnetic Loading
Unit cell size (mm)	35.4 × 35.4	6.0 × 6.0
Substrate thickness (mm)	0.952	0.824
Permittivity	1.044	15.81
Permeability	1.00	2.79
Percent bandwidth	1.67%	8.33%

The unit cell geometries and reflection phase response for both designs are shown in Figure 1. It has been suggested in [8] that magnetic loading can be used as a means to increase the bandwidth of a mushroom-shape EBG structure. The design approach presented here is based on a similar strategy, but replaces the overly complicated mushroom structure with that of a planar FSS screen, thereby eliminating the need for vias. Furthermore, by using a GA to evolve single-band or multiband AMC surface designs for maximum bandwidth, the optimum values of μ and ε for such structures can be obtained.

Two examples of GA-optimized ultrathin EBG absorbers with magnetic substrates are also presented in this section. The first design is optimized for absorption at 6 GHz, with a maximum thickness of 1 mm. The goal in this design is to obtain a better bandwidth than the conventional ultrathin absorber presented in [5]. The geometry of this GA optimized absorber is shown in Figure 2. Metal is represented by the black pixels, while the absence of metal is indicated by a white pixel. The corresponding frequency response of both the reflection coefficient magnitude and phase are shown in Figures 3 (a) and 3(b), respectively. It is crucial to note here that the absorber response is best at the AMC condition, where the phase of the reflection coefficient passes through zero degrees.

To compare this result with the previous example given in [5], an overlay of the two magnitude responses versus frequency is shown in Figure 4. The dimensions of the two designs are provided in Table 2. The new absorber with magnetic substrate has a dielectric value that dominates the magnetic value, consistent with available substrate materials. With any practical magnetic substrate material used in this frequency range, the intrinsic permittivity will be much larger than the

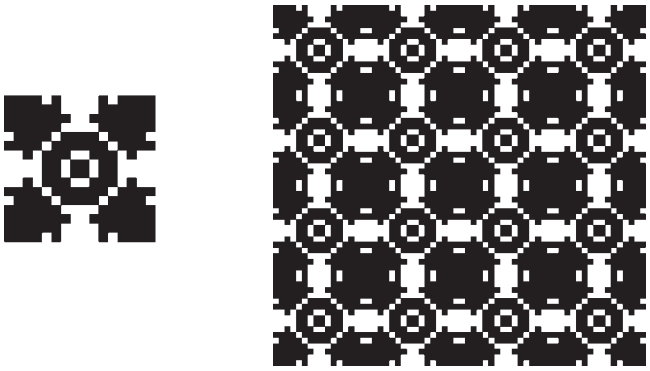

Figure 5 Unit cell geometry and corresponding FSS screen geometry for an additional ultrathin electromagnetic bandgap absorber with magnetic substrate

permeability. By examining Figure 4, it can be seen that the bandwidths of these two designs are quite different. This is due to the magnetic loading of the substrate for the second design. Thus, this new design is superior to previous electromagnetic absorbers because for any required bandwidth, the magnetic substrate absorber will be considerably thinner. Moreover, given a minimum absorber thickness, the magnetic substrate design will have a larger operating bandwidth. For either application, the performance of the magnetic loaded absorber is superior to its unloaded counterpart.

The next design presented was optimized for a thinner EBG absorber with the same bandwidth near 6 GHz. Figure 5 shows the unit cell and screen geometries for this design. The reflection magnitude and phase angle versus frequency are shown in Figure 6, where it can be seen that the resonant frequency is obtained at approximately 5.9 GHz. It is important to note that the thickness of this new design is 0.48 mm, whereas the original design without magnetic loading has a total thickness of 0.952 mm. The other parameters for this design are listed in Table 3.

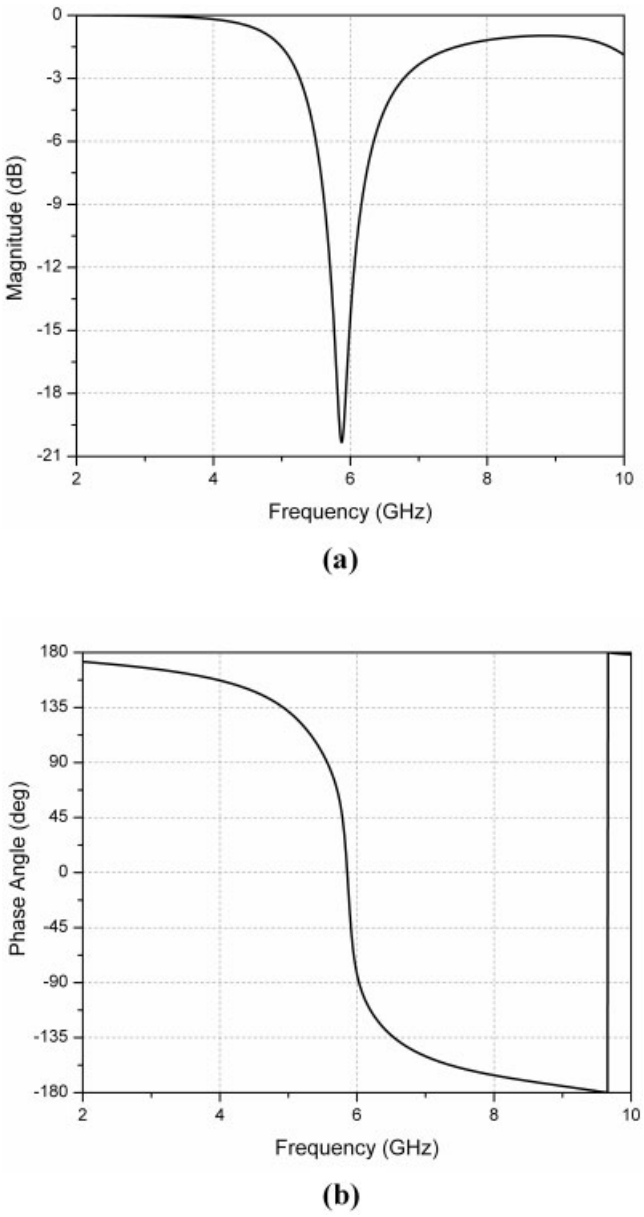

Figure 6 Frequency response of the ultrathin EBG absorber near 6 GHz. Reflection coefficient magnitude versus frequency (a), and reflection phase angle versus frequency (b)

TABLE 3 Design Parameters for the Thinner Magnetically Loaded 6-GHz EBG Absorber

Unit cell size (mm)	3.81 × 3.81
Substrate thickness (mm)	0.48
Permittivity	19.22
Permeability	2.87
Percent bandwidth	5.60%

4. CONCLUSION

A new method has been introduced for incorporating reasonable amounts of magnetic loss into the substrate of EBG AMC surfaces (ground planes) and ultrathin EBG absorbers to increase the bandwidth and reduce the thickness respectively. It has been demonstrated that magnetic loading can be used to increase the bandwidth of multiband AMC surfaces for each operating frequency. Two examples of magnetic loading in EBG absorbers are also provided to show that it is possible to further reduce the thickness of previous absorber designs while maintaining the same desired bandwidth of operation. By utilizing the metaferrite equivalence of such an EBG structure to a PEC backed magnetic slab, it is possible to obtain effective absorber designs with reduced thickness or increased bandwidth.

REFERENCES

1. D.J. Kern, D.H. Werner, A. Monorchio, L. Lanuzza, and M.J. Wilhelm, The design synthesis of multiband artificial magnetic conductors using high impedance frequency selective surfaces, IEEE Trans Antennas Propag 53 (2005), 8–17.
2. A.K. Bhattacharyya and D.L. Sengupta, Radar cross section analysis and control, Artech, Boston, MA, 1991.
3. K.J. Vinoy and R.M. Jha, Radar absorbing materials: From theory to design and characterization, Kluwer, Boston, MA, 1996.
4. N. Engheta, Thin absorbing screens using metamaterial surfaces, Proc IEEE AP-S/URSI Symp Dig 2 (2002), 392–395.
5. D.J. Kern and D.H. Werner, A genetic algorithm approach to the design of ultra-thin electromagnetic bandgap absorbers, Microwave Opt Technol Lett 38 (2003), 61–64.
6. D.J. Kern, D.H. Werner, and M. Lisovich, Metaferrites: Using electromagnetic bandgap structures to synthesize metamaterial ferrites, IEEE Trans Antennas Propag 53 (2005), 1382–1389.
7. D.J. Kern, D.H. Werner, and P.L. Werner, Optimization of multi-band AMC surfaces with magnetic loading, Proc IEEE AP-S/URSI Symp Dig 1 (2004), 20–25.
8. R. Diaz, V. Sanches, E. Caswell, and A. Miller, Magnetic loading of artificial magnetic conductors for bandwidth enhancement, Proc IEEE AP-S/URSI Symp Dig 2 (2003), 431–434.